☙

Observation of Correlations Up To the Micrometer Scale in Sliding Charge-Density Waves

D. Le Bolloc'h,[1] V. L. R. Jacques,[1,3] N. Kirova,[1] J. Dumas,[2] S. Ravy,[3] J. Marcus,[2] and F. Livet[4]

[1]*Laboratoire de Physique des Solides (CNRS-UMR 8502), Bâtiment 510, Université Paris-sud, 91405 Orsay cedex, France*
[2]*Institut Néel, CNRS/UJF, BP166 38042 Grenoble cedex 9, France*
[3]*Synchrotron SOLEIL, L'Orme des merisiers, Saint-Aubin BP 48, 91192 Gif-sur-Yvette cedex, France*
[4]*Sciences et Ingénierie des Matériaux et Procédés, INP Grenoble CNRS UJF, BP 75, 38402 St Martin d'Hères Cedex, France*

A high resolution coherent x-ray diffraction experiment has been performed on the charge-density wave (CDW) system $K_{0.3}MoO_3$. The $2k_F$ satellite reflection associated with the CDW has been measured with respect to external dc currents. In the sliding regime, the $2k_F$ satellite reflection displays secondary satellites along the chain axis which corresponds to correlations up to the micrometer scale. This super long-range order is 1500 times larger than the CDW period itself. This new type of electronic correlation seems inherent to the collective dynamics of electrons in charge-density wave systems. Several scenarios are discussed.

PACS numbers: 71.45.Lr

Ferroelectrics, magnetic systems, liquid crystals, spin, and charge-density waves (CDWs) may stabilize incommensurate structures with the underlying lattice [1]. In most cases, the stability of incommensurate modulations relies upon a coupling with the underlying lattice or intrinsic defects. The case of charge-density waves is particular because the electronic modulation is mainly driven by the electronic structure. The nesting of the Fermi surface stabilizes the modulation and the band filling fixes the wave vector of the modulation at twice the Fermi wave vector $2k_F$, which may be incommensurate. The $K_{0.3}MoO_3$ blue bronze system, for example, stabilizes an incommensurate charge-density wave modulation at $2k_F = 0.748 \pm 0.001$ [2] along the chain axis.

This incommensurate $2k_F$ wave vector has a well-known consequence: the invariance by translation allows the electronic crystal to slide over the underlying lattice for currents greater than a threshold value. The signature of this sliding motion has been mainly observed by transport measurements [3,4]: a large broad band noise is observed, as well as periodic voltage oscillations [5,6].

Observing the collective dynamics of electrons by classical diffraction has always been a significant challenge. The task is difficult in CDW systems because the CDW's domains are usually larger than the micrometer scale and any translational motion does not change the diffraction pattern. Only a few consequences of the sliding have been observed by using high-resolution x-ray diffraction, as, for example, the loss of transverse coherence of CDW domains [7], the contraction of the CDW close to electrical contacts [8], or its rotation around a step [9]. By using high-resolution and coherent x-ray diffraction, we show in this Letter a novel consequence of the sliding CDW and the incommensurate $2k_F$ wave vector: a super long-range order, up to the micrometer scale, appears in the sliding regime of the CDW. This observation, as well as an earlier one reported in [10], became possible only by using coherent microdiffraction.

We have studied the blue bronze which is a classic CDW system. This is a quasi-1D structure, made of clusters of 10 MoO_6 octahedra, forming chains along the [010] direction ($b = 7.56$ Å), and layers along the [102] direction. The reciprocal vector $\mathbf{b}^*$ runs along the chains and $2\mathbf{a}^*$-$\mathbf{c}^*$ is perpendicular to the layers. Let $\mathbf{u}(\mathbf{r}) = \mathbf{u}_0 \cos(\mathbf{q}_c \cdot \mathbf{r} + \Phi(\mathbf{r}))$ be the periodic lattice distortion in quadrature with the CDW, where $\mathbf{q}_c = (1, 2k_F, \overline{0.5})$ is defined as the wave vector normal to the CDW wave fronts. At equilibrium, the CDW exhibits intrinsic defects like dislocations [10,11] and displays its own vibration modes [12,13]. The dispersion curve of the CDW acoustic mode, the so-called phason mode, which is responsible for the sliding motion of the CDW as a whole, has been measured by inelastic neutron scattering [12].

We used the same high quality single crystal as in our previous experiment [10]. Its electrical resistance has been carefully measured before and after the experiment. In both cases, a pronounced decrease of the differential resistance was observed at the threshold current, accompanied by a rapid increase of the broadband noise, which is a signature of the sliding state. The transition temperature ($T_c = 183$ K) and the threshold current ($I_s = 1.2$ mA at 75 K) remained unchanged after the experiment: x rays did not alter the macroscopic CDW's properties. No heating effect under the x-ray beam has been observed.

The coherent x-ray diffraction experiment has been performed at the ID01 beam line at the ESRF. The $0.5 \times 2 \times 0.2$ mm^3 sample was mounted in a top-loading cryostat cooled down to 75 K with He exchange gas. The sample was initially aligned with the $\mathbf{b}^*$ axis vertical, and the $2\mathbf{a}^*$-$\mathbf{c}^*$ axis in the horizontal scattering plane. The patterns were recorded on a direct illuminated CCD camera (22 μm $\times$ 22 μm pixel size) located 1.20 m from the sample position. The beam quality and its transverse coherence length were tested by closing the entrance slit at 2 μm $\times$ 2 μm: the expected crosslike diffraction pattern was observed with strong contrast of fringes [14].

The degree of coherence can be estimated from the experimental setup around 10% [15]. The penetration depth was 18 μm^{-1} and the footprint of the x-ray beam on the sample's surface was 45 μm (the incident angle equals 12.6°). In this study, the main interest of using a coherent beam is the small beam size and the excellent Q resolution. A resolution of $\delta q = 0.7 \times 10^{-4}$ Å^{-1} along $\mathbf{b}^*$ (i.e., $\delta q = 0.8 \times 10^{-4}$ in $\mathbf{b}^*$ units.) was achieved at 7.5 keV ($\lambda = 1.65$ Å) by using 10 $\mu m \times 10$ μm entrance slits.

The experiment consisted of recording the 2D diffraction patterns of the $\mathbf{Q}_s = (5, \bar{1}, \bar{3}) + \mathbf{q}_c$ satellite reflection and the $(6, 0, \bar{3})$ fundamental Bragg peak, far from any electric contact. Both reflections have been measured successively after each current variation. Because of the experimental geometry, the 2D reciprocal plane probed by the CCD at the satellite angle corresponds to the $(\mathbf{b}^*, \mathbf{t}^*)$ plane, where $\mathbf{t}^*$ is the direction tilted by 19.5° from the $2\mathbf{a}^*$-$\mathbf{c}^*$ direction [16]. Several CCD acquisitions have been recorded for different incident θ angles, with $\delta\theta = 10^{-3}$ degree steps. This allows us to get the three dimensional intensity distribution of the reflections (see Fig. 1). In this way, the behavior of the $2k_F$ reflection and the main Bragg reflection was observed with respect to external current, especially along the chain direction $\mathbf{b}^*$ and the transverse direction $2\mathbf{a}^*$-$\mathbf{c}^*$. In order to get more intensity, we have integrated the volume of Fig. 1 over the θ axis. The corresponding 2D pattern is displayed without current in Fig. 1(c) and with current in Fig. 1(d). The 2D patterns
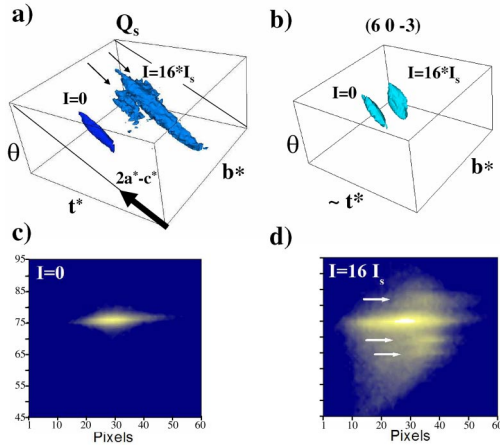
shown in Fig. 2 correspond to a section of Fig. 1 along the $2\mathbf{a}^*$-$\mathbf{c}^*$ direction through the $2k_F$ reflection.

First, the host lattice seems to be insensitive to the applied current: the $(6, 0, \bar{3})$ fundamental Bragg peak remains unchanged under the applied current within the experimental resolution [Fig. 1(b)]. On the other hand, the CDW modulation displays original features for large enough currents. Under current, a broadening of the $2k_F$ reflection is observed along the $2\mathbf{a}^*$-$\mathbf{c}^*$ transverse direction which corresponds to decreasing CDW correlation lengths from $\xi_t = 1.2$ μm at $I = 0$ mA to $\xi_t = 0.6$ μm at $I = 12$ I_s and to $\xi_t = 0.4$ μm at $I = 16$ I_s [Fig. 2(d)]. The loss of the transverse order under external currents, along the softest direction of blue bronze [17], has already been observed in several studies [7].

The most striking feature appears along the $\mathbf{b}^*$ direction. Without current, the $2k_F$ reflection displays a single peak, the width of which corresponds to the entrance slit aperture: the CDW's domain is larger than 10 μm along $\mathbf{b}^*$. Above approximately 12 times the threshold current, the Q_s satellite starts to broaden along $\mathbf{b}^*$ [Fig. 2(b)]. This broadening increases continuously for larger currents. At a current 16 times larger than the threshold, several maxima located at regular positions along $\mathbf{b}^*$ are clearly distinguished from the $2k_F$ reflection [see Fig. 1(d)]. All of them display approximately the same width, slightly larger than the $2k_F$ width without current. As shown in Fig. 1, these new intensity maxima correspond to well-defined 3D peaks and will be called secondary satellite reflections in the following. These secondary satellite reflections are located at $(6, \overline{0.252} \pm n\delta q_s, \overline{3.5})$ with $\delta q_s = 4.9 \times 10^{-4}$ $\mathbf{b}^*$ units [see Figs. 1(a), 1(d), 2(c), and 2(e)]. The reduced wave vector δq_s leads to a period of $L = 2\pi/\delta q_s = 1.5$ μm.
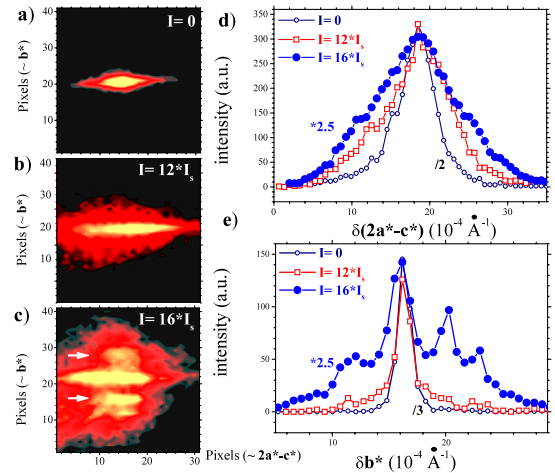

FIG. 1 (color online). 3D diffraction patterns of (a) the $Q_s = (6, \overline{0.252}, \overline{3.5})$ satellite and (b) the $(6, 0, \bar{3})$ fundamental Bragg reflection for two current values at $T = 75$ K. Each isosurface has been fixed at $I_{\max}/18$ for the $(6, 0, \bar{3})$ and $I_{\max}/7$ for Q_s. For clarity, the reflections with and without current have been shifted along $\mathbf{b}^*$. The total size of the boxes is $40 \times (\delta\theta = 10^{-3}$ degree) (vertical axis) by 50×60 pixels (horizontal plane). Each 3D acquisition lasted less than 15 mn. 2D patterns corresponding to integration of the Fig. 1(a) over the θ axis, without (c) and with current (d). The secondary satellites are indicated by arrows.

FIG. 2 (color online). 2D diffraction patterns (30×40 pixels) of the $2k_F$ reflection in the $(2\mathbf{a}^*$-$\mathbf{c}^*; \mathbf{b}^*)$ plane for $I = 0$ mA (a), $I = 12$ I_s (b), and $I = 16$ I_s (c). The secondary satellites are indicated by arrows. Corresponding profiles along $2\mathbf{a}^*$-$\mathbf{c}^*$ in (d) and $\mathbf{b}^*$ in (e). The profiles have been rescaled.

We did not increase the current further for fear of destroying the electrical contacts. The appearance of secondary satellite reflections is reversible: after heating up the sample above T_c under zero field and cooling down to 75 K again, the same diffraction pattern has been observed [18]. These secondary satellite reflections were also observed in a second high quality crystal. Note the strong intensity of higher-order satellites and the asymmetry of the profile in Fig. 2(e) [19]. Figure 1(d) also displays an asymmetric diffuse intensity along the transverse direction. This is surely due to inhomogeneities in the CDW current density within the probed volume. Those inhomogeneities have been observed by transport measurements in the blue bronze [6]. We also noticed the absence of any speckle on either the $2k_F$ reflection or on secondary satellites, despite the coherence properties of our x-ray beam. This last point will be brought up later.

Let us discuss the interpretation. First, the secondary satellites cannot be due to the fragmentation of CDW in isolated CDW's domains, 1.5 μm wide along **b***. The truncation effect due to finite CDW's domains would lead to very weak satellites with respect to the main $2k_F$ reflection. It cannot be explained either by the presence of a single CDW dislocation as it has been observed in blue bronze without current in [10]. Indeed, the distance between each fringe would be constant whatever the current and equal to the beam size, i.e., $\delta q = 2\pi/10$ μm $= 0.6 \times 10^{-4}$ Å^{-1}. In addition, the main $2k_F$ reflection should disappear because of the presence of the dislocation. The last two points are in contradiction with our measurement. Finally, phase shifts randomly distributed in the volume would lead to typical speckle patterns [20] and not to regular satellite reflections as observed in Fig. 1(d). Note also that purely dynamical phenomena, like phase slips, would only have a negligible effect on the $2k_F$ reflection.

We interpret the experimental data as due to a long-range periodic structure which modulates the CDW state along **b***. This super long-range order is surprising since the period L is 1500 times larger than the CDW period along the chain direction ($\lambda_{CDW} \approx 4/3b = 10.08$ Å). To our knowledge, long-range electronic correlations up to the micrometer scale have never been observed in electronic systems.

The existence of this super long-range order is a direct consequence of the incommensurability of the $2k_F$ wave vector and of the sliding motion of the electronic crystal. Several scenarios are briefly discussed here, based on static or dynamic phenomena: a soliton lattice, an ordering of CDW dislocations, or a new vibration mode induced by sliding.

The observed periodic sequence of satellites flanking the $2k_F$ reflection displays a remarkably high and slowly decaying intensity. It signifies the appearance under current of nonharmonic periodic structure, modulating the CDW state along **b***. An amplitude modulation of the CDW

would yield symmetrical secondary satellite reflections, that only structure factor or Debye-Waller effects could make asymmetric in intensity. On the other hand, a phase modulation would directly result in asymmetric secondary satellite reflections [1,21]. This remark, along with the well-known fact that phase excitations cost much less energy than amplitude ones, leads us to consider this latter case in the following.

Consider first a long-range modulation provided by a static soliton lattice. In blue bronzes, the CDW wave vector ($Q = 0.748$**b***) is close to 0.750**b*** corresponding to the quarterization along the chain. The actual crystallographic space group requires an 8-order commensurability ($8\mathbf{q_c}$ is a fundamental Bragg reflection) which locks the CDW phase φ at multiples of $\pi/4$ via the energy $\sim -\alpha \cos(8\varphi)$ [22]. Thus, the proximity to the commensurability point results in a lattice of discommensurations, or solitons with the phase increment $\Delta\varphi = \pi/4$. The soliton lattice is characterized by the soliton size l and the distance between the solitons L. The single soliton size $l \sim (C/\alpha)^{1/2}$ is then determined jointly by the energy α and the CDW longitudinal elastic modulus C. At low applied current the preexisting soliton lattice corresponds to an almost sinusoidal phase, and manifests itself as the pure shift of the CDW peak without secondary satellites. At higher applied currents, however, a strong decrease of elastic modulus C (corresponding to a decreasing l) leads to nonharmonic modulation of the phase φ and to higher-order satellites at $2\pi/L$ as in Fig. 2(e). The strong variation of C necessary to get a nonharmonic modulation could be due to a screening effect by free carriers. In any case, the existence of the soliton lattice allows the electronic crystal to approach the commensurate modulation. In this work, however, we did not observe any clear shift of the $2k_F$ reflection toward 0.75**b*** under current. Note that this mechanism is based on the interaction between the CDW and the underlying lattice, without taking explicitly into account the presence of extrinsic defects [23].

Another explanation of the secondary satellites could be the presence of an array of CDW edge dislocations. A single CDW dislocation has already been observed in the bulk in [10]. They can be formed below the surface due to the charge transfer or other types of stress near the surface. In the sliding state but for moderate electric field, the randomly distributed dislocations can still be pinned, leading to a mere change of the $2k_F$ profiles [24]. At high electric fields, the CDW dislocations can be depinned and form a periodic structure. Correlated dislocations of the host lattice are known in crystals stressed by the epitaxial layers (see, for example, [25]). The above model corresponds also to a nonharmonic modulation and leads to higher-order satellites and to an asymmetric profile.

As already mentioned in the introduction, the secondary satellites have been observed several times. We never observed speckles but smooth profiles, despite the coher-

ence properties of our x-ray beam. The absence of any speckle is a strong indication that this phenomenon could also have a dynamic origin. The secondary satellites could be the consequence of the presence of a propagating mode, associated with the sliding of the condensate. An estimate of the frequency of the mode without current can be obtained by extrapolating, at δq_s, the phason dispersion curve measured by inelastic neutron scattering [12]. For $\delta q_s = 4.9 \times 10^{-4}$ in $\mathbf{b}^*$ units, one obtains frequencies in the gigahertz range (15 GHz at 175 K and approximately 4 times larger at 75 K), i.e., a particularly low frequency mode. In the sliding state, a softening of this phason mode at δq_s could explain the observed data since the diffracted intensity is inversely proportional to the frequency squared of the vibration mode. The origin of the very soft mode remains to be clarified.

In conclusion, electronic correlations up to micrometer scale are observed, along the chain axis, in the sliding regime of the blue bronze by using coherent x-ray diffraction. However, the appearance of super long-range correlations induced by CDW motion is still difficult to understand. Several scenarios are presented, based on the ordering of topological defects (solitons, edge dislocations) or the softening of a phason mode. Additional experiments are necessary to clarify the origin of this phenomenon.

[1] For a review, see H. Z. Cummins, Phys. Rep. **185**, 211 (1990).

[2] J.-P. Pouget, C. Noguera, A. H. Moudden, and R. Moret, J. Phys. (France) **46**, 1731 (1985); J.-P. Pouget, in Ref. [3], p. 87.

[3] For a review on the blue bronze, see *Low Dimensional Electronic Properties of Molybdenum Bronzes and Oxides*, edited by C. Schlenker (Klüwer Academic, Dordrecht, 1989).

[4] For a review, see *Charge Density Waves in Solids*, edited by L. P. Gor'kov and G. Grüner (North-Holland, Amsterdam, 1989).

[5] R. M. Fleming and C. C. Grimes, Phys. Rev. Lett. **42**, 1423 (1979); Z. Z. Wang, M. C. Saint Lager, P. Monceau, M. Renard, P. Gressier, A. Meeschaut, L. Guemas, and J. Rouxel, Solid State Commun. **46**, 325 (1983).

[6] P. Beauchêne, J. Dumas, A. Janossy, J. Marcus, and C. Schlenker, Physica (Amsterdam) **143B+C**, 126 (1986); M. F. Hundley and A. Zettl, Phys. Rev. B **39**, 3026 (1989).

[7] T. Tamegai *et al.*, Solid State Commun. **51**, 585 (1984); R. M. Fleming, R. G. Dunn, and L. F. Schneemeyer, Phys. Rev. B **31**, 4099 (1985).

[8] D. DiCarlo, E. Sweetland, M. Sutton, J. D. Brock, and R. E. Thorne, Phys. Rev. Lett. **70**, 845 (1993); S. Brazovskii, N. Kirova, H. Requardt, F. Ya. Nad, P. Monceau, R. Currat, J. E. Lorenzo, G. Grübel, and Ch. Vettier, Phys. Rev. B **61**, 10 640 (2000); H. Requardt, F. Ya. Nad, P. Monceau, R. Currat, J. E. Lorenzo, S. Brazovskii, N. Kirova, G. Grübel, and Ch. Vettier, Phys. Rev. Lett. **80**, 5631 (1998).

[9] Y. Li, S. G. Lemay, J. H. Price, K. Cicak, K. O'Neill, K. Ringland, K. D. Finkelstein, J. D. Brock, and R. E. Thorne, Phys. Rev. Lett. **83**, 3514 (1999); A. F. Isakovic, P. G. Evans, J. Kmetko, K. Cicak, Z. Cai, B. Lai, and R. E. Thorne, Phys. Rev. Lett. **96**, 046401 (2006).

[10] D. Le Bolloc'h, S. Ravy, J. Dumas, J. Marcus, F. Livet, C. Detlefs, F. Yakhou, and L. Paolasini, Phys. Rev. Lett. **95**, 116401 (2005).

[11] P. A. Lee and T. M. Rice, Phys. Rev. B **19**, 3970 (1979).

[12] B. Hennion, J. P. Pouget, and M. Sato, Phys. Rev. Lett. **68**, 2374 (1992); J. P. Pouget, B. Hennion, C. Escribe-Fillipini, and N. Sato, Phys. Rev. B **43**, 8421 (1991).

[13] S. Ravy, H. Requardt, D. Le Bolloc'h, P. Foury-Leylekian, J.-P. Pouget, R. Currat, P. Monceau, and M. Krisch, Phys. Rev. B **69**, 115113 (2004).

[14] I. K. Robinson, R. Pindak, R. M. Fleming, S. B. Dierker, K. Ploog, G. Grubel, D. L. Abernathy, and J. Als-Nielsen, Phys. Rev. B **52**, 9917 (1995); D. Le Bolloc'h, F. Livet, F. Bley, T. Schulli, M. Veron, and T. H. Metzger, J. Synchrotron Radiat. **9**, 258 (2002).

[15] F. Livet, Acta Crystallogr. Sect. A **63**, 87 (2007).

[16] The scheme of the reciprocal lattice can be found in our previous article [10].

[17] In blue bronze, the constant force along the $2\mathbf{a}^*$-$\mathbf{c}^*$ direction is 100 times weaker than along $\mathbf{b}^*$ (see [12]).

[18] Memory effects are well known in blue bronze. A virgin state is obtained by increasing the temperature above T_c and by cooling down without current.

[19] We have also observed that the whole $2k_F$ profile was shifted along $\mathbf{b}^*$ for some current values. We consider that this global shift is mainly due to the finite reproducibility of the diffractometer since the $(6, 0, \bar{3})$ and the $2k_F$ reflections have been measured successively after each current variation. We can estimate that the shifts of the $2k_F$ profile with respect to the current, if any, remain less than $\delta q = 10^{-3}$ Å$^{-1} \sim 2.5 \times \delta q_s$.

[20] To see typical speckle pattern at wide angles, see, for example, S. Ravy, D. Le Bolloc'h, R. Currat, A. Fluerasu, C. Mocuta, and B. Dkhil, Phys. Rev. Lett. **98**, 105501 (2007).

[21] R. A. Cowley, Adv. Phys. **29**, 1 (1980).

[22] P. A. Lee, T. M. Rice, and P. W. Anderson, Solid State Commun. **14**, 703 (1974).

[23] For another model of CDW sliding without interactions with defects see S. Aubry and P. Quemerais in [3], p. 295.

[24] N. Kirova and S. Brazovskii, J. Phys. IV (France) **131**, 147 (2005).

[25] G. Renaud, P. Guenard, and A. Barbier, Phys. Rev. B **58**, 7310 (1998).